Differential Geometry of Monogenic Signal Representations*

Lennart Wietzke[1], Gerald Sommer[1], Christian Schmaltz[2], and Joachim Weickert[2]

[1] Institute of Computer Science, Chair of Cognitive Systems, Christian-Albrechts-University of Kiel, Germany
[2] Faculty of Mathematics and Computer Science, Mathematical Image Analysis Group, Saarland University, Saarbrücken, Germany

Abstract. This paper presents the fusion of monogenic signal processing and differential geometry to enable monogenic analyzing of local intrinsic 2D features of low level image data. New rotational invariant features such like structure and geometry (angle of intersection) of two superimposed intrinsic 1D signals will be extracted without the need of any steerable filters. These features are important for all kinds of low level image matching tasks in robot vision because they are invariant against local and global illumination changes and result from one unique framework within the monogenic scale-space.

Key words: Low-level Image Analysis, Differential Geometry, Geometric (Clifford) Algebra, Monogenic Curvature Tensor, Monogenic Signal, Radon Transform, Riesz Transform, Hilbert Transform, Local Phase Based Signal Processing

1 Introduction

Local image analysis is the first step and therefore very important for detecting key points in robot vision. One aim is to decompose a given signal into as many as possible features. In low level image analysis it is necessary not to loose any information but to be invariant against certain features in which two similar key points are allowed to differ, i.e. two crossing lines (see figure 1) can have different main orientations in two images which have to be matched but they should have the same structure (phase) and apex angle (angle of intersection) in both images. The local phase $\varphi(t)$ of an assumed signal model $\cos(\varphi(t))$ and the apex angle of two superimposed signals are rotational invariant features of images and therefore very important for matching tasks in robot vision. Two superimposed patterns are of big interest being analyzed because they are the most frequently (after intrinsic 0D and 1D signals) appearing 2D structures in images. In this paper we present how to decompose 2D image signals which consist locally of two

* We acknowledge funding by the German Research Foundation (DFG) under the projects *SO 320/4-2* and *We 2602/5-1*.

intrinsical 1D signals. To extract the essential features like the main orientation, the apex angle and the phase of those signals no heuristics will be applied in this paper like in many other works [Stuke2004] but a fundamental access to the local geometry of two superimposed 1D signals will be given. This paper will be the first step and provides also the grasp to analyze an arbitrary number of superimposed signals in future work. In the following 2D signals $f \in \mathcal{L}_2(\Omega, \mathbb{R})$

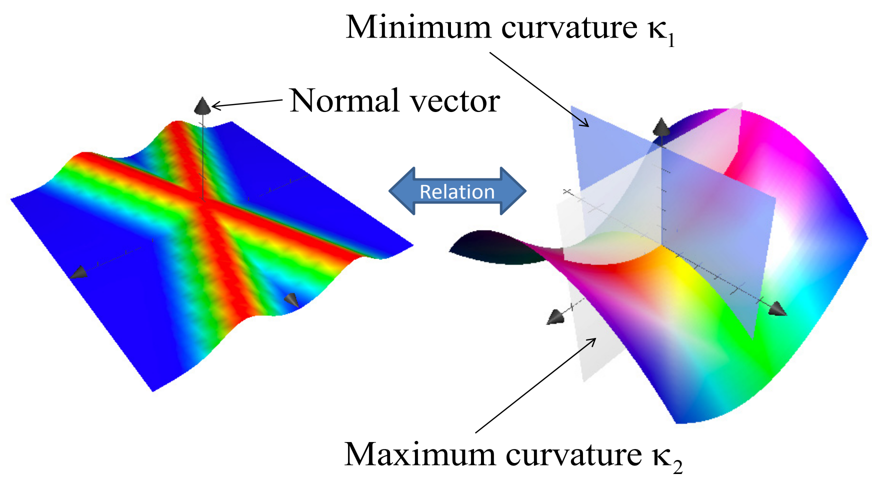

Fig. 1. This figure illustrates the relation of signal processing and differential geometry in $\mathbb{R}^3$. Images will be visualized in their Monge patch embedding with the normal vector of the tangential plane being always at the point of origin $(0, 0) \in \mathbb{R}^2$. From left to right: The image pattern in Monge patch embedding and its corresponding assumed local curvature saddle point model. Note that the normal section in direction of the two superimposed lines has zero curvature in the image pattern as well as in the curvature model.

will be analyzed in the Monge patch embedding (see figure 1) $I_f = \{x\mathbf{e}_1 + y\mathbf{e}_2 + f(x, y)\mathbf{e}_3 | (x, y) \in \Omega \subset \mathbb{R}^2\}$ which is well known from differential geometry with $\{1, \mathbf{e}_1, \mathbf{e}_2, \mathbf{e}_3, \mathbf{e}_{12}, \mathbf{e}_{13}, \mathbf{e}_{23}, \mathbf{e}_{123}\}$ as the set of basis vectors of the Clifford algebra $\mathbb{R}_3$ [Porteous1995]. A 2D signal f will be classified into local regions $N \subseteq \Omega$ of different intrinsic dimension (also known as codimension):

$$f \in \begin{cases} \text{i0D}_N,\ f(\mathbf{x}_i) = f(\mathbf{x}_j)\ \forall \mathbf{x}_i, \mathbf{x}_j \in N \\ \text{i1D}_N,\ f(x, y) = g(x \cos\theta + y \sin\theta)\ \forall (x, y) \in N, g \in \mathbb{R}^{\mathbb{R}}, f \notin \text{i0D}_N \\ \text{i2D}_N,\ \text{else} \end{cases} \tag{1}$$

The set of signals being analyzed in this work can be written as the superposition of two i1D signals such as two crossing lines or a checkerboard:

$$\bigcup_{N\subseteq \Omega}\left\{ f \in \mathcal{L}_2(\Omega,\mathbb{R}) | f(\mathbf{x}) = \sum_{i\in\{1,2\}} f_i(\mathbf{x}) \; \forall \mathbf{x} \in N, f_i \in \mathrm{i1D}_N \right\} \subset \mathrm{i2D} \qquad (2)$$

The set of i1D signals can be completely analyzed by the monogenic signal [Felsberg2001] which splits the signal locally into phase, orientation and amplitude information. Two superimposed i1D signals with arbitrary main orientation and phase can be analyzed by the structure multivector [Felsberg2002] with the significant restriction that the two signals must be orthogonal, i.e. their apex angle must be fixed to 90°. Recently the monogenic curvature tensor has been introduced by [Zang2007] to decompose i2D signals into main orientation and phase information. Proofs and an exact signal model have not been given. This paper refers to [Felsberg2002,Felsberg2004,Zang2007] and fuses monogenic signal processing with differential geometry to analyze two superimposed i1D signals. The results of this work will be proofs concerning the monogenic curvature tensor and in addition the exact derivation of the apex angle (angle of intersection between two crossing lines) without the use of any heuristic. Future work will contain analysis of an arbitrary number of superimposed i1D signals.

1.1 The 2D Radon Transform

In this paper the monogenic signal [Felsberg2001] and the monogenic curvature tensor [Zang2007] will be interpreted in Radon space which gives beautiful access to analyzing the concatenation of Riesz transforms of any order. Remember that the Riesz transform of a 2D signal can be interpreted as the well known Hilbert transform of 1D signals within the Radon space. Therefore all odd order Riesz transforms (i.e. the concatenation of an odd number of Riesz transforms) apply a one dimensional Hilbert transform to multidimensional signals in a certain orientation which is determined by the Radon transform [Beyerer2002]. The Radon transform is defined as:

$$r := r(t,\theta) := \mathcal{R}\{f\}(t,\theta) := \int_{(x,y)\in\Omega} f(x,y)\delta_0(x\cos\theta + y\sin\theta - t)d(x,y) \qquad (3)$$

with $\theta \in [0..\pi)$ as the orientation, $t \in \mathbb{R}$ as the minimal distance of the line from the origin and δ_0 as the delta distribution (see figure 2). The inverse Radon transform exists and is defined by:

$$\mathcal{R}^{-1}\{r(t,\theta)\}(x,y) := \frac{1}{2\pi^2}\int_{\theta=0}^{\pi}\int_{t\in\mathbb{R}} \frac{1}{x\cos\theta + y\sin\theta - t}\frac{\partial}{\partial t} r(t,\theta)dtd\theta \qquad (4)$$

The point of interest where the phase and orientation information should be obtained within the whole signal will always be translated to the origin $(0,0)$ for each point $(x,y) \in \Omega$ so that the inverse Radon transform can be simplified to:

$$\mathcal{R}^{-1}\{r\}(0,0) = -\frac{1}{2\pi^2}\sum_{i\in I}\int_{t\in\mathbb{R}} \frac{1}{t}\frac{\partial}{\partial t} r(t,\theta_i)dt \qquad (5)$$

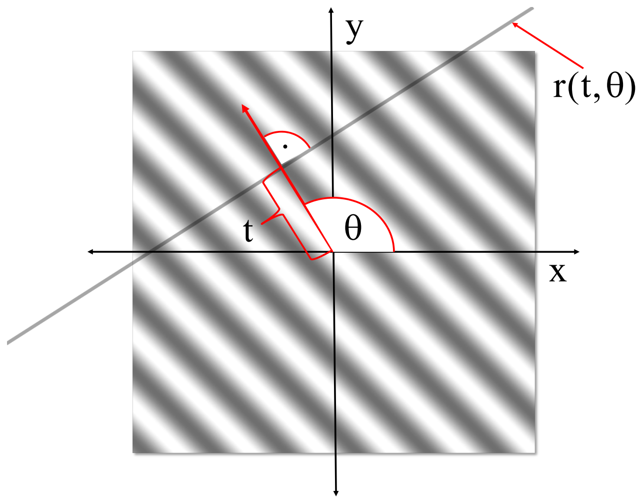

Fig. 2. All the values lying on the line defined by the distance t and the orientation θ will be summed up to define the value $r(t,\theta)$ in the Radon space.

This simplification is an important new result because the integral of the θ can be replaced by the finite sum of discrete angles θ_i to enable modeling the superposition of an arbitrary number of i1D signals. The integral of θ vanishes because of the fact that $r(t_1,\theta) = r(t_2,\theta)\ \forall t_1,t_2 \in \mathbb{R}\ \forall\theta \in [0..\pi) - \bigcup_{i\in I}\{\theta_i\}$ implies $\frac{\partial}{\partial t} r(t,\theta) = 0\ \forall t \in \mathbb{R}\ \forall\theta \in [0..\pi) - \bigcup_{i\in I}\{\theta_i\}$ for a finite number $|I| \in \mathbb{N}$ of superimposed i1D signals which build the i2D signal $f = \sum_{i\in I} f_i$ where each single i1D signal f_i has its own orientation θ_i. Note that in this work we restrict the set of signals to $|I| = 2$.

2 Interpretation of the Riesz Transform in Radon Space

The Riesz transform $R\{f\}$ extends the function f to a monogenic (holomorphic) function. The Riesz transform is a possible but not the only generalization of the Hilbert transform to a multidimensional domain and reads:

$$R\{f\}(x,y) = \begin{bmatrix} R_x\{f\}(x,y) \\ R_y\{f\}(x,y) \end{bmatrix} = \begin{bmatrix} \frac{x}{2\pi(x^2+y^2)^{\frac{3}{2}}} * f(x,y) \\ \frac{y}{2\pi(x^2+y^2)^{\frac{3}{2}}} * f(x,y) \end{bmatrix} \quad (6)$$

(with $*$ as the convolution operation). The Riesz transform can be also written in terms of the Radon transform:

$$R\{f\}(x,y) = \mathcal{R}^{-1}\{h_1(t) * r(t,\theta) n_\theta\}(x,y) \quad (7)$$

with $n_\theta = [\cos\theta, \sin\theta]^T$ and h_1 as the one dimensional Hilbert kernel in spatial domain. Applying the Riesz transform to an i1D signal with orientation θ_m

results in:

$$\begin{bmatrix} R_x\{f\}(0,0) \\ R_y\{f\}(0,0) \end{bmatrix} = \underbrace{\left[-\frac{1}{2\pi^2} \int_{t\in\mathbb{R}} \frac{1}{t} h_1(t) * \frac{\partial}{\partial t} r(t,\theta_m) dt \right]}_{=:s(\theta_m)} n_{\theta_m} \tag{8}$$

Note that $\frac{\partial}{\partial t}(h_1(t) * r(t,\theta)) = h_1(t) * \frac{\partial}{\partial t} r(t,\theta)$. The orientation of the signal can therefore be derived by:

$$\arctan \frac{R_y\{f\}(0,0)}{R_x\{f\}(0,0)} = \arctan \frac{s(\theta_m)\sin\theta_m}{s(\theta_m)\cos\theta_m} = \theta_m \tag{9}$$

(see also figure 3). The Hilbert transform of f and with it also the one dimensional phase can be calculated by:

$$\sqrt{[R_x\{f\}(0,0)]^2 + [R_y\{f\}(0,0)]^2} = (h_1 * f_{\theta_m})(0) \tag{10}$$

with the partial Hilbert transform [Hahn1996] $(h_1 * f_\theta)(0) = -\frac{1}{\pi} \int_{\tau\in\mathbb{R}} \frac{f(\tau\cos\theta, \tau\sin\theta)}{\tau} d\tau$. The first order Riesz transform of any i2D signal consisting of a number $|I|$ of

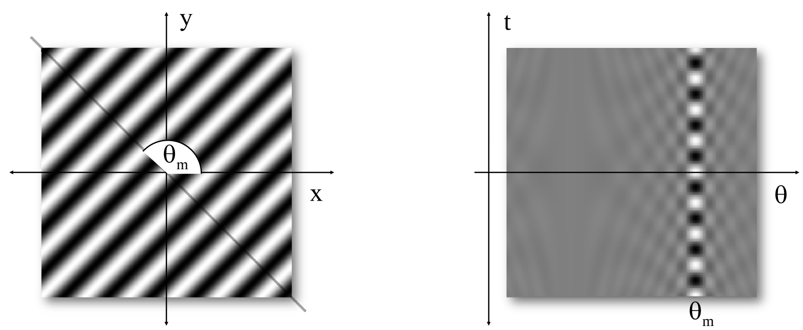

Fig. 3. From left to right: i1D signal in spatial domain with x- and y-axis and with main orientation θ_m and in Radon space with θ- and t-axis. Even though in the right figure some artifacts can be seen in the Radon space, those artifacts do not exist in case of an infinite support of the image patterns and therefore the artifacts will be neglected in this work: $\frac{\partial}{\partial t} r(t,\theta) = 0 \; \forall t \; \forall \theta \neq \theta_m$ and in the left figure $r(t_1,\theta) = r(t_2,\theta) \; \forall t_1, t_2 \; \forall \theta \neq \theta_m$

i1D signals therefore reads:

$$\begin{bmatrix} R_x\{f\}(0,0) \\ R_y\{f\}(0,0) \end{bmatrix} = \sum_{i\in I} \underbrace{\left[-\frac{1}{2\pi^2} \int_{t\in\mathbb{R}} \frac{1}{t} h_1(t) * \frac{\partial}{\partial t} r(t,\theta_i) dt \right]}_{=:s(\theta_i)} n_{\theta_i} = \sum_{i\in I} s(\theta_i) n_{\theta_i} \tag{11}$$

With the assumption that e.g. two superimposed i1D signals have arbitrary but same phase the main orientation θ_m of the resulting i2D signal can be calculated:

$$s := s(\theta_1) = s(\theta_2) \Rightarrow \begin{bmatrix} R_x\{f\}(0,0) \\ R_y\{f\}(0,0) \end{bmatrix} = s \begin{bmatrix} \cos\theta_1 + \cos\theta_2 \\ \sin\theta_1 + \sin\theta_2 \end{bmatrix} \tag{12}$$

$$\Rightarrow \arctan \frac{R_y\{f\}(0,0)}{R_x\{f\}(0,0)} = \frac{\theta_1 + \theta_2}{2} = \theta_m \tag{13}$$

The most important conclusion of this result is that the monogenic signal can be used not only to interpret i1D signals but also to calculate the main orientation of the superposition of two and more i1D signals which construct the complex i2D signals.

3 Analyzing the Monogenic Curvature Tensor

Recently the monogenic curvature tensor has been introduced by [Zang2007] to extend the monogenic signal to analyze also i2D signals. It has been shown that the monogenic curvature tensor already contains the monogenic signal. Roughly spoken the monogenic curvature tensor has been motivated by the concept of the Hessian matrix of differential geometry and so far has only been known in Fourier domain. This drawback makes interpretation hard when applying the monogenic curvature tensor to a certain signal model with explicit features such like orientation, apex angle and phase information. Instead, this problem can be solved by the analysis of the spatial domain of the Riesz transform. Now any i2D signal will be regarded as the superposition of a finite number of i1D signals $f = \sum_{i \in I} f_i$. With the properties $\mathcal{R}\{\mathcal{R}^{-1}\{r\}\} = r$ and $\mathcal{R}\{\sum_{i \in I} f_i\} = \sum_{i \in I} \mathcal{R}\{f_i\}$ [Toft1996] and because of $h_1 * h_1 * f = -f$ the even part of the monogenic curvature tensor T_e can be also written in terms of the concatenation of two Riesz transforms and therefore also in terms of the Radon transform and its inverse [Stein1970]:

$$T_e(f) := \mathcal{F}^{-1}\left\{\mathcal{F}\{f\}(\alpha,\rho)\begin{bmatrix} \cos^2\alpha & -\sin\alpha\cos\alpha\mathbf{e}_{12} \\ \sin\alpha\cos\alpha\mathbf{e}_{12} & \sin^2\alpha \end{bmatrix}\right\} = \tag{14}$$

$$= \begin{bmatrix} R_x\{R_x\{f\}\} & -R_x\{R_y\{f\}\}\mathbf{e}_{12} \\ R_x\{R_y\{f\}\}\mathbf{e}_{12} & R_y\{R_y\{f\}\} \end{bmatrix} \tag{15}$$

With $\mathcal{F}\{f\}(\alpha,\rho)$ as the Fourier transform of the signal f in polar coordinates with α as the angular component and ρ as the radial component and $\mathcal{F}^{-1}$ as the inverse Fourier transform. To understand the motivation of the monogenic curvature tensor please compare the even Tensor $T_e(f)$ with the well known Hessian matrix:

$$M_{\text{Hesse}}(f) := \begin{bmatrix} f_{xx} & -f_{xy}\mathbf{e}_{12} \\ f_{xy}\mathbf{e}_{12} & f_{yy} \end{bmatrix} \tag{16}$$

where the partial derivative of the signal f simply have been replaced by the corresponding Riesz transforms. Now as a new result of this work the even tensor in Radon space reads:

$$T_e(f) = -\begin{bmatrix} \mathcal{R}^{-1}\{\cos^2\theta\mathcal{R}\{f\}\} & -\mathcal{R}^{-1}\{\sin\theta\cos\theta\mathcal{R}\{f\}\}\mathbf{e}_{12} \\ \mathcal{R}^{-1}\{\sin\theta\cos\theta\mathcal{R}\{f\}\}\mathbf{e}_{12} & \mathcal{R}^{-1}\{\sin^2\theta\mathcal{R}\{f\}\} \end{bmatrix} \tag{17}$$

The advantage of this form is that the signal features such like the orientation θ is explicitly given. In the Fourier form the orientation is not given. So with the previous results of the Radon interpretation of the Riesz transform the features of the signal can be easily extracted. For the sake of completeness the odd tensor is defined as the Riesz transform of the even tensor:

$$T_o(f) = T_e(R_x\{f\} + R_y\{f\}\mathbf{e}_{12}) \tag{18}$$

So the monogenic curvature tensor can be written as $T(f) = T_e(f) + T_o(f)$. Only the even part T_e of the monogenic curvature tensor T will be used in the following.

3.1 Interpretation of Two Superimposed i1D Signals

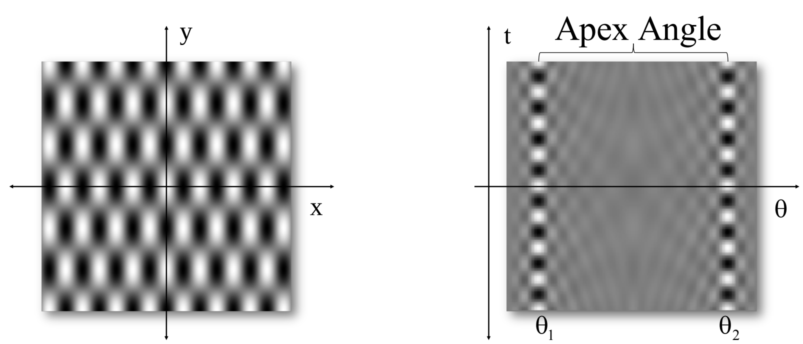

Fig. 4. From left to right: Two superimposed i1D signals with orientation θ_1 and θ_2 in spatial domain and in Radon space. Assuming that both signals have same phase φ the signal information can be separated by the Riesz transform.

In the following two superimposed i1D signals with orientations θ_1, θ_2 and arbitrary but same phase φ for both i1D signals will be analyzed in Radon space (see figure 4). With the abbreviations: $a := \cos\theta_1,\ b := \cos\theta_2,\ c := \sin\theta_1,\ d := \sin\theta_2$ the even tensor for two superimposed i1D signals reads:

$$T_e = f(0,0)\begin{bmatrix} a^2 + b^2 & -(ca + db)\mathbf{e}_{12} \\ (ca + db)\mathbf{e}_{12} & c^2 + d^2 \end{bmatrix} \tag{19}$$

According to differential geometry the well known Gaussian curvature $K := \kappa_1\kappa_2$ and the main curvature $H := \frac{1}{2}(\kappa_1 + \kappa_2)$ can be also defined for the even tensor. Both features are rotational invariant. Motivated by differential geometry it will be shown how to compute the apex angle as an important rotational invariant feature of i2D signals by means of the Gaussian and the main curvature of the even tensor.

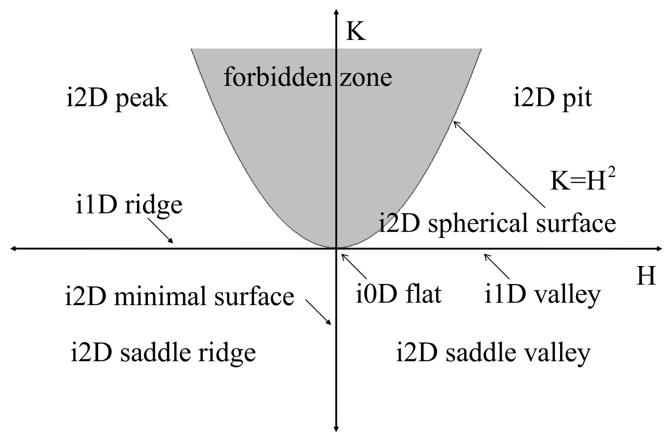

Fig. 5. Classification of local image models by Gaussian and mean curvatures.

3.2 The Apex Angle in Terms of Surface Theory in $\mathbb{R}^3$

The apex angle can be calculated indirectly by means of the two orthogonal main curvatures κ_1, κ_2 of a surface. Actually a surface at a certain point can have an infinite number of different 1D curvatures or only one unique curvature. This will be explained in detail. Differential geometry considers a certain point with certain differentiable properties. In the following this will be fulfilled only at the infinite small region of that point in the assumed saddle point curvature model (see figure 5). But the region around a point of interest in the image data can not assumed to be infinite small. This difference of curvature model and the true image data is very important for the following argument. At the point of interest the normal vector of the tangential plane and another arbitrary point which is not part of the normal vector span a plane which can be rotated around the normal vector by any angle. That plane is used to intersect the two dimensional image surface I_f to deliver a one dimensional function which has a well defined curvature at that point for every angle. This generated set is called normal section (see figure 6). To analyze two superimposed i1D structures their intersection point will be approximated by a local i2D saddle point model (see figure 1). This local model describes the pattern up to the sign of the maximum curvature which will not affect the results of the global image model. So when adjusting the global i2D structure the minimum curvature κ_1 and the maximum curvature κ_2 of the local curvature model now lie on the x-axis and on the y-axis. Because of that the normal cut curvature in directions of the two principal axes delivers the minimum and the maximum curvature of the local i2D saddle point model (see figure 7). Remember that in direction of the i1D structures the normal cut curvature is zero. So if it is possible to determine the angle where the curvature is zero the apex angle could be calculated. This can be done by

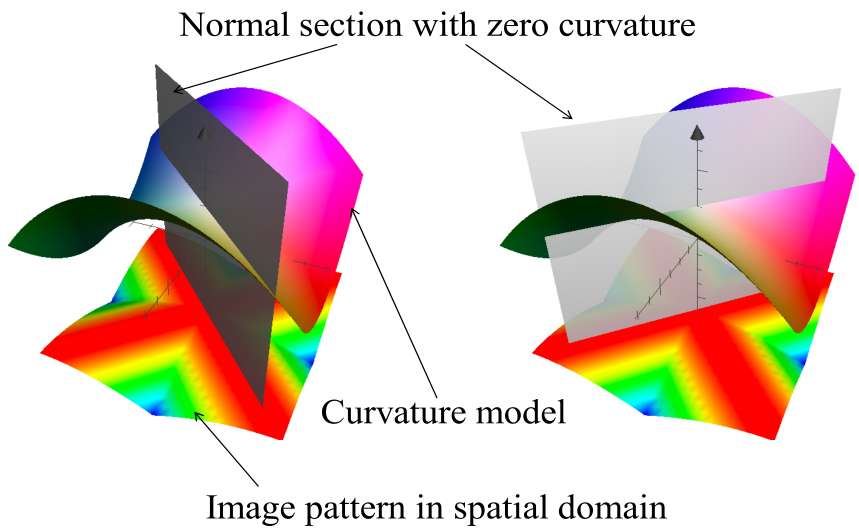

Fig. 6. The curvature of the normal section is zero iff the present structure is of intrinsically one dimension in direction of the section plane.

applying the results of Euler's and Meusnier's theorems (see [Baer2001], p.104).

$$\kappa\left(\frac{\alpha}{2}\right) = \lim_{f_{xy}(0,0)\to 0} \kappa_1 \cos^2\frac{\alpha}{2} + 2f_{xy}(0,0)\sin\frac{\alpha}{2}\cos\frac{\alpha}{2} + \kappa_2 \sin^2\frac{\alpha}{2} \tag{20}$$

Here $\frac{\alpha}{2}$ is the angle between the normal section direction with minimum curvature κ_1 and the normal section direction with curvature $\kappa\left(\frac{\alpha}{2}\right)$. In general two different solutions exist. Because of that two superimposed i1D signals can be described by this local saddle point model. Since the i1D information has zero curvature and the local saddle point model assumption with $\kappa_1 < 0$ and $\kappa_2 > 0$ the apex angle can be calculated by minimal information given by κ_1 and κ_2.

$$\kappa\left(\frac{\alpha}{2}\right) = 0 \Rightarrow \alpha = 2\arctan\sqrt{\frac{|\kappa_1|}{|\kappa_2|}} \tag{21}$$

With the abbreviations $a := \cos\theta_1,\ b := \cos\theta_2,\ c := \sin\theta_1,\ d := \sin\theta_2$ the apex angle of two i1D signals can now be derived by the Gaussian curvature $K := \det(T_e) = [f(0,0)]^2\,(a^2d^2 + b^2c^2 - 2abcd)$ and the main curvature $H := \frac{1}{2}\mathrm{trace}(T_e) = \frac{1}{2}(a^2+b^2+c^2+d^2)f(0,0) = f(0,0)$ in a rotational invariant way.

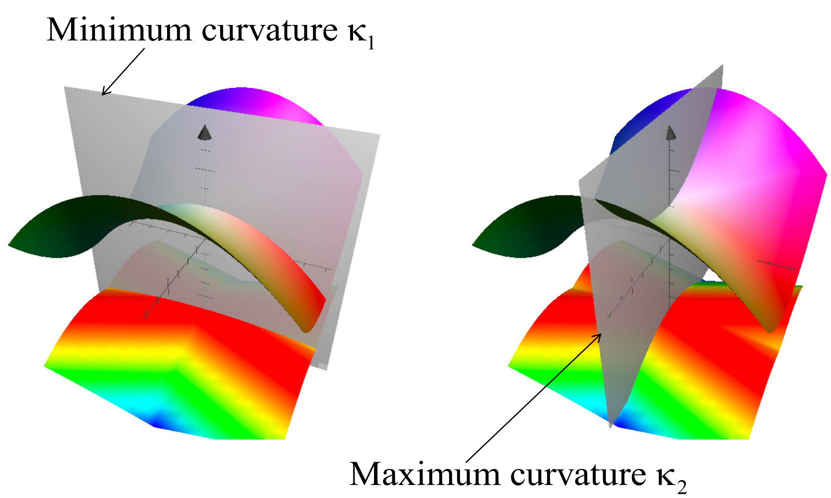

Fig. 7. The normal sections of the bisectors along the principal x-axis (left figure) and the principal y-axis (right figure) are analyzed to determine the apex angle α.

This yields the apex angle:

$$\left|\frac{\theta_1 - \theta_2}{2}\right| = \arctan\sqrt{\left|\frac{H - \sqrt{H^2 - K}}{H + \sqrt{H^2 - K}}\right|} \tag{22}$$

4 Experiments and Results

For the synthetic i2D signal consisting of two crossing lines (see figure 8) the following model is used

$$f_{\theta_1,\theta_2}(x, y) := \max\left\{e^{-(x\cos\theta_1 + y\sin\theta_1)^2}, e^{-(x\cos\theta_2 + y\sin-\theta_2)^2}\right\} \tag{23}$$

which will be analyzed at the origin $(0, 0)$. To analyze the apex angle by the even part of the monogenic curvature tensor the following synthetic checkerboard signal (see figure 8) will be used:

$$f_{\theta_1,\theta_2}(x, y) := \frac{1}{2}\left[\cos\left[(x\cos\theta_1 + y\sin\theta_1)\pi\right] + \cos\left[(x\cos\theta_2 + y\sin\theta_2)\pi\right]\right] \tag{24}$$

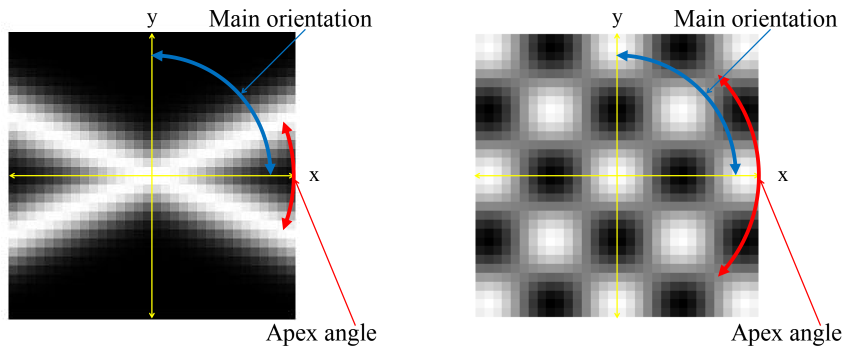

Fig. 8. Discrete synthetic i2D signals with different apex angles. From left to right: Two crossing i1D lines and the i2D checkerboard.

The average angular error will be defined by:

$$\mathrm{AAE} := \sum_{\theta_1=0^\circ}^{45^\circ} \sum_{\theta_2=0^\circ}^{45^\circ} \left| |\theta_1 - \theta_2| - 2\arctan\sqrt{\left|\frac{H-\sqrt{H^2-K}}{H+\sqrt{H^2-K}}\right|}\right|^2 \tag{25}$$

with $H := \frac{1}{2}\mathrm{trace}(T_e(f_{\theta_1,\theta_2}))$ and $K := \det(T_e(f_{\theta_1,\theta_2}))$. The experimental AAE of the checkerboard signal is 0.067° and 0.08° for the two crossing lines with total convolution mask size $(2*8+1)^2$. The AAE converges to 0° with increasing convolution mask sizes. Also the main orientation of an arbitrary number of superimposed i1D signals can be computed on discrete signals without any error with increasing convolution mask sizes.

5 Conclusion and Future Work

The odd-order Riesz transform of any i1D or i2D signal can be analyzed in Radon space in which a one dimensional partial Hilbert transform will be applied in direction of each i1D signal with its individual orientation θ_i, $i \in I$. Assuming that two superimposing i1D signals have arbitrary but same phase φ, the orientations θ_1, θ_2 and the phase can be calculated. The advantage of analyzing the Riesz transform in Radon space is that the signal properties consisting of orientation and phase are explicitly given after applying the general operator (e.g. the monogenic curvature operator) to the specific i1D or i2D signal function. Future work will include analyzing the superposition of i1D signals with individual phases φ_i. Note that arbitrary but same phase of both signals has been assumed in this paper for deriving the main orientation and the apex angle, so that only one common phase can be calculated by this assumption. The analysis of i2D signals in Radon space presented in this work realizes to interpret the monogenic curvature tensor for the first time in an exact way.
Future work will contain investigation of the promising isomorphism $M(2, \mathbb{R}_3) \cong$

$\mathbb{R}_{4,1}$ [Sobczyk2005] from the set of the monogenic curvature tensors to the set of the multivectors of the conformal space in Radon space.

References

[Baer2001] Christian Baer, Elementare Differentialgeometrie, de Gruyter, Vol 1, Berlin, New York, 2001

[Beyerer2002] Jürgen Beyerer and Fernando Puente Leon, The Radon transform in digital image processing, Oldenbourg, 2002, Vol 50, Part 10, pages: 472-480, Automatisierungstechnik, Germany

[Felsberg2001] Michael Felsberg and Gerald Sommer, The monogenic signal, IEEE Transactions on Signal Processing, 49(12):3136-3144, December 2001

[Felsberg2002] Michael Felsberg, Low-Level Image Processing with the Structure Multivector, PhD Thesis, Kiel University, 2002

[Felsberg2004] Michael Felsberg and Gerald Sommer, The monogenic scale-space: A unifying approach to phase-based image processing in scale-space, Kluwer Academic Publishers, 21:5-26, 2004

[Hahn1996] S.L. Hahn, Hilbert Transforms in Signal Processing, Artech House, Norwood, Maryland, 1996

[Porteous1995] Ian R. Porteous, Clifford Algebras and the Classical Groups, Cambridge Studies in Advanced Mathematics, Cambridge University Press, 1995

[Sobczyk2005] Garret Sobczyk and Gordon Erlebacher, Hybrid matrix geometric algebra, H. Li, P. J. Olver and G. Sommer (Eds.): IWMM-GIAE 2004, LNCS 3519, pp. 191-206, Springer-Verlag Berlin Heidelberg, 2005

[Stein1970] Elias M. Stein, Singular Integrals and Differentiability Properties of Functions, Princeton Mathematical Series, Princeton University Press, Princeton, New Jersey, 1970

[Stuke2004] I. Stuke, T. Aach, E. Barth and C. Mota, Analysing superimposed oriented patterns, Image Analysis and Interpretation, 6th IEEE Southwest Symposium on Volume, Pages: 133-137, 2004

[Toft1996] Peter Toft, The Radon Transform - Theory and Implementation, PhD Thesis, Department of Mathematical Modelling, Technical University of Denmark, 1996

[Zang2007] Di Zang and Gerald Sommer, Signal modeling for two-dimensional image structures, Journal of Visual Communication and Image Representation, vol. 18(1), pages 81-99, 2007